Excitons in nanoscale systems

Nanoscale systems are forecast to be a means of integrating desirable attributes of molecular and bulk regimes into easily processed materials. Notable examples include plastic light-emitting devices and organic solar cells, the operation of which hinge on the formation of electronic excited states, excitons, in complex nanostructured materials. The spectroscopy of nanoscale materials reveals details of their collective excited states, characterized by atoms or molecules working together to capture and redistribute excitation. What is special about excitons in nanometre-sized materials? Here we present a cross-disciplinary review of the essential characteristics of excitons in nanoscience. Topics covered include confinement effects, localization versus delocalization, exciton binding energy, exchange interactions and exciton fine structure, exciton–vibration coupling and dynamics of excitons. Important examples are presented in a commentary that overviews the present understanding of excitons in quantum dots, conjugated polymers, carbon nanotubes and photosynthetic light-harvesting antenna complexes.

GREGORY D. SCHOLES*[1] AND GARRY RUMBLES[2]

[1]Department of Chemistry 80 St George Street, Institute for Optical Sciences, and Centre for Quantum Information and Quantum Control, University of Toronto, Toronto, Ontario M5S 3H6, Canada
[2]National Renewable Energy Laboratory, Chemical and Biosciences Center, MS3216, 1617 Cole Boulevard, Golden, Colorado 80401-3393, USA
*e-mail: gscholes@chem.utoronto.ca

An exciting aspect of nanoscience is that relationships between structure and electronic properties are being revealed through a combination of synthesis, structural characterization, chemical physics and theory. Spectroscopy is a tool that is sensitive to aspects of the electronic structure of materials. As such, spectroscopic studies of nanoscale systems often provide insights into the collective absorption and redistribution of excitation energy. This vibrant field is the study of excitons in nanoscale systems. These electronic excitations differ from excitons in bulk materials, and represent a distinct class of exciton that can be thought of either as a confined bulk-type exciton or a molecular excitation. In this review for the non-specialist, our aim is to capture the essence of the field and highlight areas of current interest. For the expert, we aim to provoke cross-disciplinary discussion and emphasize some of the challenges at the leading edge of the field. Overall we aim to identify and discuss characteristic features of excitons in materials with nanometre-size dimensions or organization. Part of our emphasis is to highlight topics at the forefront of the field, and to suggest questions that should be asked in future work.

Excitons can be formed by association of electrical charge units (free carriers) or by direct photoexcitation. The exciton luminescence that can follow this charge association underlies organic light-emitting diode technologies[1]. Conversely, excitons that are formed readily by photoexcitation can dissociate into free carriers (unbound electrons and holes) and thus play a central role in photovoltaic and solar cell devices[2]. Excitons that remain bound and emit light can be used as laser media[3]. These observations help to illustrate the concept of excitons compared with free carriers in bulk materials[4]. Photoexcitation creates an electron in the conduction band, leaving a 'hole' in the valence band. If the interaction between the electron and hole is assumed to be negligible—justified when each wavefunction is spread over an expanse of atoms—then the pair are free carriers. On the other hand, an attractive coulombic interaction between the electron and hole 'quasi-particles' binds them into an exciton. A distinguishing feature of excitons is that the spatial extent of an electronic excited state is increased through coherent sharing of the excitation among subunits of the material. That characteristic is determined by electronic coupling among the repeat units that make up the material[5–8].

Excitons in nanoscale systems are formed by light absorption in molecules such as polyacenes and polyenes, conjugated polymers, quantum dots, molecular aggregates, carbon nanotubes and so on. The new aspect of excitons that is prevalent in, or

even defines, nanoscience is that the physical size and shape of the material strongly influences the nature and dynamics of the electronic excitation. Therefore, a deciding property of excitons in nanoscale systems is that the exciton size is dictated not by the electron–hole Coulomb interaction, but by the physical dimensions of the material or the arrangement of distinct building blocks. That interests the chemist because excitons can be engineered in a material according to structure. It is of interest to physicists because the spatial confinement of the exciton accentuates many of its interesting physical properties, exposing them for examination. The theorist may conclude that perhaps we should not try to force-fit existing theories to model excitations in nanostructures as they often carry with them assumptions that we have forgotten, or that we erroneously ignore. Nanoscale materials thus provide both a testbed and an inspiration for new quantum mechanical approaches to the calculation of electronic properties of large systems. Through the study of excitons in nanoscale systems we are learning some general rules defining how size and shape tunes electronic structure and dynamics. In Fig. 1 a summary of excitons in bulk materials (adapted from ref. 6) is extended to indicate how excitons in nanoscale systems differ. An overview and introduction to elements of excitons in nanoscale systems is given in Box 1.

A challenge in this field is that the materials under investigation are often complex; they contain many atoms, they can be structurally disordered or influenced by surface effects, and samples often have an inhomogeneous composition in terms of structural disorder and size polydispersity. We attempt below to provide some insights into how such hurdles have been overcome. Questions being addressed include: can the properties of confined excitons be used to change the way that solar cells or lasers operate? How should we transfer the language of solid-state physics to organic systems[9], and vice versa?

A unifying theme in nanoscience is that size and shape are important. How best can we understand and compare nanomaterials and the implications of size-tunable properties for excitons? A powerful approach is to combine experiment and theory. However, owing to the intermediate length scales characteristic of many nanomaterials, unique challenges for theory are presented. For example, the huge number of electrons presents difficulties for molecular-type electronic structure calculations,

Box 1: An introduction to excitons in nanoscale systems

1. Bands and molecular orbitals for extended systems
Periodic, strongly coupled molecular or atomic systems are characterized by a high density of delocalized orbitals that form the valence (VB) and conduction (CB) bands. Those bands can be represented in real space as shown on the left side of the diagram, or equivalently, the energy of each band can be plotted against its wave vector k, as in the right schematic. Excitation of an electron from VB to CB creates free carriers. The minimum energy required is that of the bandgap, E_g.

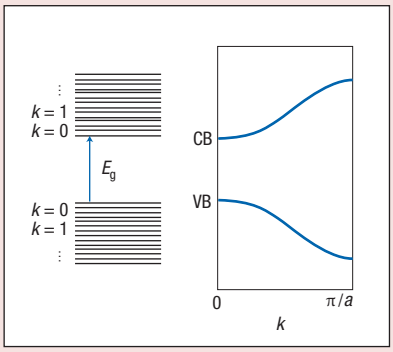

2. Excitons in extended systems: bound electron–hole pairs
The language that describes the features of the quasi-particle approach is nicely intuitive. An exciton in a spatially entended system is described as a neutral excitation particle: an electron–hole pair. In an exciton the electron and hole are bound by the electron-hole Coulomb interaction. In the chemist's electron–electron language, the 'attraction' derives from decreased electron–electron repulsion integrals in the excited state configuration compared with the ground state, thus lowering the energy of that configuration relative to the continuum by the exciton binding energy, $E_b = E_g - E_x$. Related electron–hole exchange interactions mix the Hartree–Fock (single particle) configurations, so that the exciton states are finally obtained through a configuration interaction (CI-singles) calculation. Correct spin eigenstates can only be obtained by antisymmetrizing wavefunctions and mixing configurations through exchange interactions.

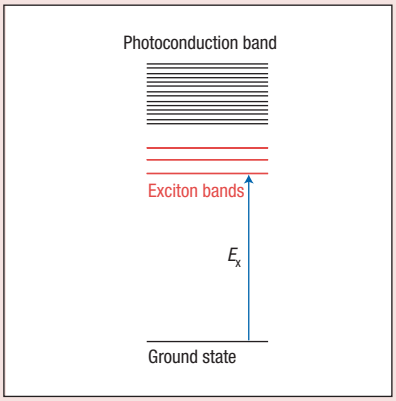

Box 1: Continued

3. Molecular orbital picture for confined systems
Occupied (in the ground state) and virtual molecular orbitals for a series of polyacenes. As the conjugation size increases, the bandgap decreases and the density of states increases. These quantum size effects derive from changes in electron–electron interactions that are proportional to molecular orbital wavefunction delocalization. A single-excitation configuration is constructed by excitation of an electron from an occupied to a virtual orbital. That configuration is delocalized over the extent of the molecule. However, to be consistent with the definition of an exciton in an extended system, the change in electron–electron interactions after excitation needs to be considered to describe the exciton. The single-excitation configurations are mixed by exchange interactions so that each excited state — exciton state — is a linear combination of the single-excitation configurations. A manifold of singlet and triplet excitons are thus obtained.

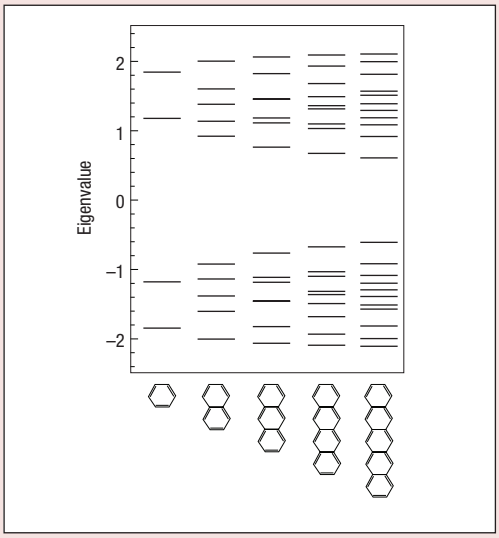

4. Spectroscopy of molecular excitons
Absorption spectra of a series of naphthyl dimer molecules[117] compared with a monomeric model chromophore (dashed line). The dimer spectra consist of two bands, with a splitting equal to the electronic coupling H_{LR} between the naphthyl groups on the left (L) and right (R), indicating that the excitation is shared between the two chromophores: a molecular exciton. A schematic diagram of the relative energies and wavefunctions of the napthyl moieties compared to the dimer is given below. The redshift of the centre of gravity of the exciton bands is due to orbital mixing effects. These interactions induce the electron and hole to delocalize over the subunits. Model dimers such as shown here allow for detailed examination of interchromophore interactions, including realistic treatment of solvation[118]. (Spectra reprinted with permission from ref. 117. Copyright (1993) American Chemical Society).

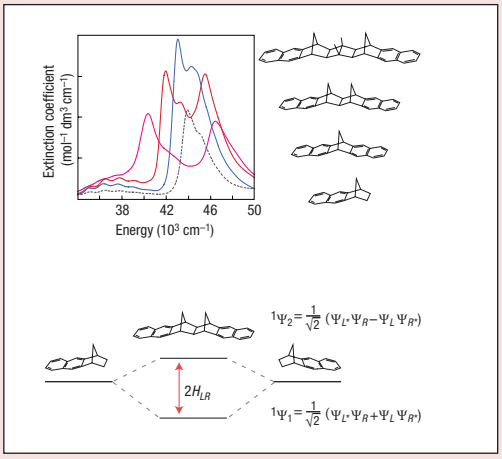

which scale steeply with the number of electrons, yet the importance of atomic-scale details needs to be captured. Great progress has been made in solving such problems, as has been reviewed elsewhere[10–13]. In this review we will cover four broad topics of importance in the spectroscopy of excitons in nanoscale systems. To illustrate the ways in which excitons in nanoscale systems are unique or interesting, and to formulate some general observations that may stimulate cross-disciplinary discussion, we will describe examples pertaining to quantum dots, conjugated polymers, carbon nanotubes and photosynthetic light-harvesting antenna complexes within each of these subject areas. We begin by providing some background on each material.

OVERVIEW OF THE MATERIALS

PHOTOSYNTHETIC LIGHT-HARVESTING COMPLEXES

Proteins organized in the photosynthetic membranes of higher plants, photosynthetic bacteria and algae accomplish the capture of incident photons (light-harvesting), subsequent spatial redistribution of that excitation energy, and the ultimate trapping of the energy via photo-induced electron transfer, with remarkably high efficiencies[14]. Suspensions of surfactant-isolated light-harvesting complexes (known as LH2) from purple bacteria provide a good example. They show two absorption bands (Fig. 2), attributed to two distinct arrangements of bacteriochlorophyll-*a* (Bchl) molecules. The B800 absorption band is due to

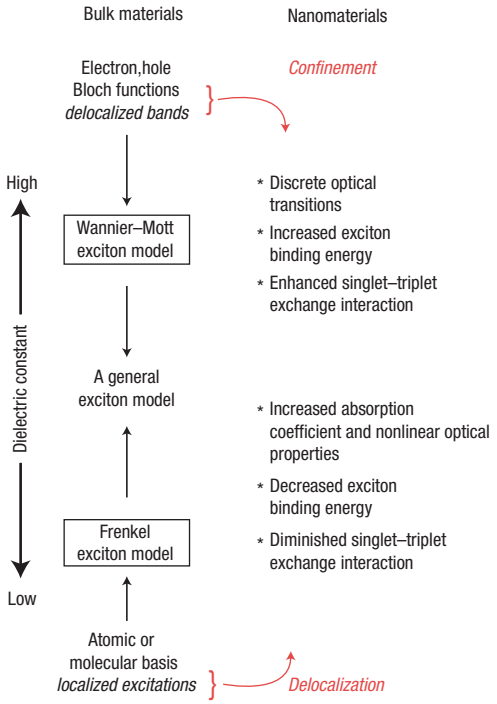

Figure 1 Excitons in nanoscale systems. The diagram relates the Wannier and Frenkel exciton models and sketches the basis for describing excitons. The description may proceed from delocalized bands, wherein the electron and hole may move freely throughout the material. Such a model can be used to model excitons in crystalline materials with high dielectric constant, such that electron–hole Coulomb interactions are small compared with the bandgap of the material. One may also develop a model starting from a localized basis set. The tight-binding model is an example of this approach. In their usual implementation, either approach contains approximations or limitations that restrict its application. A general exciton model overcomes such limitations, and contains all the key features necessary to describe the excited states of a molecule as well as an infinite system. Nanoscale excitons can be described starting from the point of view of either a delocalized or a localized excitation. In a delocalized representation of the problem, nanoscale excitons are subject to quantum confinement, and their spectroscopy becomes richer. With respect to a model based on localized functions, nanoscale materials can sustain more delocalized excitations. The Frenkel model uses the point of view, particularly useful for molecular aggregates, that the wavefunction is separable into distinct electron groups tightly associated with each repeat unit. Such an approach is applied to molecular excitons, such as a photosynthetic excitons or J-aggregates.

a ring of essentially non-interacting Bchl molecules (nearest-neighbour electronic coupling ~30 cm^{-1}). The B850 band, however, is the absorption into the optically bright exciton states characteristic of the ring of strongly interacting Bchl molecules (nearest-neighbour electronic coupling ~300 cm^{-1}). Here is an example of electronic coupling among molecules that creates a new chromophore: a Frenkel exciton. The excitons that are of interest in these systems include Frenkel excitons, but are primarily weakly coupled localized excitations[15]. Relatively weak electronic coupling amongst the many hundreds of chromophores that are bound in light-harvesting proteins enables the excitation energy to be funnelled efficiently through space to reaction centre proteins[16].

In Fig. 2 a simple light-harvesting antenna protein, PE545, is shown together with a sketch of the organization of the photosynthetic membrane of a type of cryptophyte algae[17]. Each PE545 antenna protein binds eight chromophores, as seen in the structural model. Such model systems, where we know the precise arrangement of light-absorbing molecules, have provided superb model systems for learning about molecular excitons (also known as Frenkel excitons; see Fig. 1) and electronic (resonance) energy transfer. Electronic energy transfer allows excitation energy absorbed by an antenna protein to migrate rapidly (over a few picoseconds) to the peripheral chromophores, circled in the figure, then transfer into the core antenna of one of the membrane-bound photosystems, PS I or PS II (50–100 ps). In most organisms the antenna protein is also membrane-bound. The funnelling of excitation energy to the photosynthetic reaction centres involves many tens of hops, occurring on timescales of 100 fs to 100 ps. These fast, light-initiated processes occurring in proteins isolated from photosynthetic organisms have been studied in great detail over the past years[14,17]. It has become evident that the organization of light-absorbing molecules (usually chlorophylls and carotenoids) on the nanometre length scale provides important—sometimes subtle and ingenious—optimizations that control light capture and funnelling[18].

CONJUGATED POLYMERS

Conjugated polymers are highly conjugated linear macromolecules that are of great current interest because of their semiconductor-like properties and ease of processing. Excitons in conjugated polymers such as functionalized poly(phenylene vinylene) (for example MEH-PPV, poly[2-methoxy-5-(2′-ethyl)hexyloxy-1,4-phenylene vinylene]) and alkyl polyfluorenes have been intensively studied from both experimental and theoretical viewpoints to understand their nature and dynamics. Two basic types of exciton have been identified: intrachain and interchain. The former are formed by the extended π-conjugation along sections of the polymer backbone. Interchain excitons form when two chain segments couple through space, either because the chains are near to each other in a solid film, or because the chain is folded back on itself. Thus optical properties depend strongly on the aggregation state of the polymer. Details can be found in recent reviews[19–22].

Conjugated polymer excitons play important roles in electroluminescent and photovoltaic devices, and some intriguing properties relevant to device optimization have been reported. For example, the observation of wavelength-dependent photocurrent generation in MEH-PPV was explained by analysis of quantum chemical calculations that revealed

significant changes in mixing of configuration wavefunctions of the polymer[23]. That is, the electronic make-up of higher-energy excitons differs from excitons at the optical gap in such a way that mixing with extended charge-separated states is increased. A challenge now is to elucidate a microscopic picture that explains observations of interfacial excitons in heterojunction polymer blends[24]. Evidence suggests that such excitons can reversibly dissociate into an exciplex (an excited-state hetero-complex)[25], in which the electron and hole become spatially separated. In that case the Frenkel exciton model breaks down because in the excited state electron density is transferred from one molecule to the other. Dissociation of an exciplex produces geminate ion pairs that might play important intermediate roles in electron–hole dissociation or capture processes[26].

SEMICONDUCTING SINGLE-WALL CARBON NANOTUBES

The spectroscopy of semiconducting carbon nanotubes (CNTs)[27] has been of great interest in the last few years. CNTs are formed in a great variety of sizes and types, and typically aggregate into macroscopic bundles. Until recently, the accepted description of their electronic states and spectroscopy was a simple model that neglected interactions between electrons. However, that viewpoint changed as a result of the report of bandgap fluorescence for CNTs[28], made possible by surfactant isolation of individual tubes or small bundles of tubes, thus providing samples without large bundles and ropes in which fluorescence is quenched. Although it was not immediately recognized, that observation provided clear evidence for excitons in CNTs, supporting the earlier predictions of Ando[29].

Not surprisingly, the key advance underpinning the observation of CNT exciton fluorescence was material preparation. Nonetheless, optical spectra are highly inhomogeneously broadened, as shown in Fig. 3, by a sum of contributions from a series of CNT macromolecules. A plot of excitation energy versus fluorescence emission, Fig. 3b reveals distinct peaks corresponding to a series of individual tube types[30], which in combination with simple theory has allowed assignment of the spectral features to the various chemical types and sizes of CNTs. Nanotube types are designated by the chiral index (n,m), according to how the parent graphene sheet is rolled up to form a tube[31]. The fluorescence data[30] made it possible to assign the optical transitions and elucidate their size-evolution. An interesting observation from inspection of the fluorescence spectra is that spectral linewidths are narrow, being ~30 meV at room temperature[32]; this is probably a result of exchange narrowing[33], whereby the linewidth is reduced because the delocalized exciton states average over disorder in the site energies of primitive cells.

SEMICONDUCTOR QUANTUM DOTS

Semiconductor quantum dots (QDs), or nanocrystals, are nanometre-sized crystallites that can be prepared with great tunability of size and shape through colloidal routes[34–38]. Self-assembled QDs can be formed spontaneously in a semiconductor heterostructure grown using molecular beam epitaxy[39,40]. Typically, self-assembled QDs are lens-shaped, having a diameter of tens of nanometres and a height of a few nanometres, whereas colloidal QDs are usually spherical with radii of 1 to 4 nm and contain around 200 to thousands of atoms. The most common materials studied with respect to excitons include CuCl, CdSe, CdS, CdTe, InP, PbSe and PbS. In the early 1980s it was predicted that QDs should possess discrete electronic energy levels, more like molecules than bulk semiconductors[41,42].

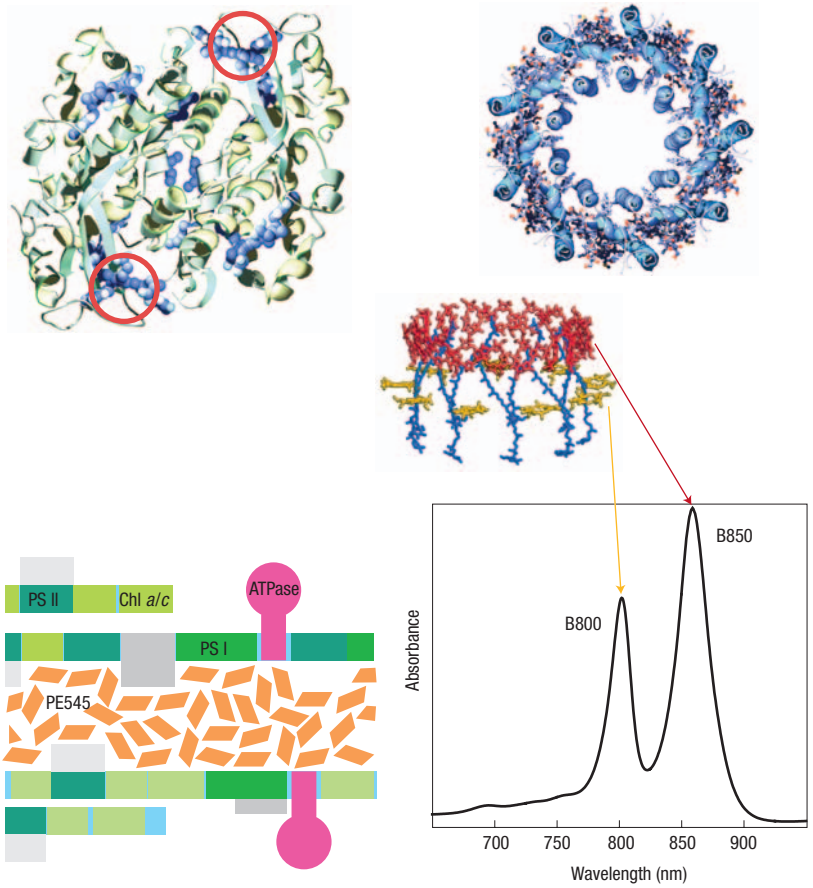

Figure 2 Frenkel excitons in photosynthesis. Left, the structure of a simple light-harvesting protein PE545 isolated from a marine cryptophyte algae. It binds eight light-absorbing molecules (blue). A cascade of electronic energy transfer steps equilibrates excitation, over timescales of tens of femtoseconds to a few tens of picoseconds, to the periphery of the protein, onto the encircled chromophores[17]. Ultimately that excitation is transferred into core antenna complexes associated with the reaction centres, photosystems I and II (PS I and PS II), organized in the thylakoid membrane as indicated schematically. (Bottom left image adapted from C. D. de Witt *et al.*, submitted to *J. Phys. Chem B.*)PE545, unlike the peripheral light-harvesting complexes of higher plants (LHC-II) or purple bacteria (LH2), is not membrane-bound. Right, the light-harvesting antenna of purple bacteria, LH2, is an example of a system whose spectroscopy is characteristic of a molecular exciton. The structural model shown at the top emphasizes the α-helices serving as a scaffold binding the light-absorbing molecules. These molecules are shown in the simplified structural model below, indicating the B850 ring (red), B800 ring (yellow) and cartenoids (blue). The absorption spectrum clearly shows the marked distinction between the B800 absorption band, arising from essentially 'monomeric' bacteriochlorophyll-*a* (Bchl) molecules, and the redshifted B850 band that is attributed to the optically bright lower exciton states of the 18 electronically coupled Bchl molecules.

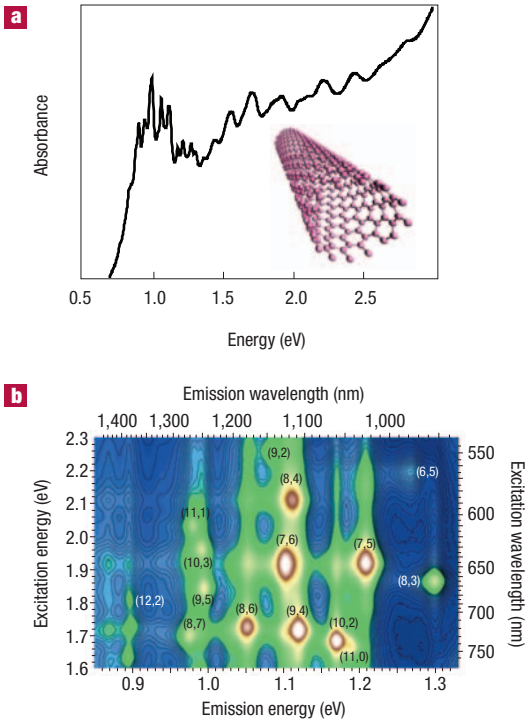

Figure 3 Excitons in single-wall carbon nanotubes. **a**, The absorption spectrum of an aqueous suspension of CNTs made by high-pressure CO conversion (HiPco), showing inhomogeneous line broadening. A single-wall CNT structural model is inset. **b**, CNT size and 'wrapping' determine the exciton energies. Samples contain many different kinds of tubes, as evident from the absorption spectrum. However, by scanning excitation wavelengths and recording a map of fluorescence spectra[30], the emission bands from various different CNTs can be discerned (see text). Assignments of the major emission peaks for this sample are indicated (T. McDonald, M. Heben & M. Jones, unpublished work; cf. ref. 32). **c**, The index (n,m) is used to define the vector $\mathbf{C}_n = n\mathbf{a}_1 + m\mathbf{a}_2$, which in turn determines the direction that the graphene sheet is rolled to form a particular CNT. The sheet is rolled so that a particular lattice point (n,m) is superimposed with (0,0).

That idea was confirmed through an accumulation of experimental work[34]. QDs are clearly differentiated from molecules in that many properties have analogues in those of bulk semiconductors, spin–orbit coupling can be significant, and they have large dielectric constants. An important consideration in deciding confinement of the exciton to the QD, in particular the size of the wavefunction compared to that of the QD, is the dielectric medium surrounding the QD[40,43]. In the coming years, shape-dependent photophysics of QD excitons will be topical, driven by recent synthetic breakthroughs[44]. Electron micrograph images of a range of CdSe QD shapes are shown in Fig. 4c–f. Nanoscale 'exciton engineering' — epiaxial growth of one semiconductor over another — opens further possibilities for improving surface passivation, changing excited state dynamics of the exciton, or manipulating wavefunctions, thereby increasing the diversity of exciton photophysics that can be examined[36].

SIZE-TUNABLE SPECTROSCOPY AND EXCITONS

What are the unique aspects of excitons in nanometre-sized materials? Certainly the prevalence of size-dependent properties is notable. A myriad of electronic properties are governed by size, including the bandgap, the exciton binding energy, and the exchange interactions. These quantities determine the spectroscopic states of the material and its (photo-)electrochemical properties. The goal of this section is to establish the spectroscopic signatures of excitons in nanoscale systems and to suggest notable aspects of their spectroscopy.

Size-tunable spectroscopic properties have been of great interest for over half a century[45], although recent interest has centred on QDs. The Bohr radius of a semiconductor exciton provides a reference as to the exciton size in the bulk. Size-tuning of properties in QDs is attributed to confinement of the exciton in a nanocrystal significantly smaller than the bulk exciton. For example, the exciton Bohr radius of PbS is ~20 nm and its bulk bandgap is 0.41 eV. Absorption spectra for PbS QDs[46] of radii ranging from ~1.3 to ~3.5 nm are shown in Fig. 5, revealing QD exciton energies in the range 0.7 to 1.5 eV.

The spectroscopic properties of molecular materials that scale in size can be elucidated in great detail, thus providing a foundation for a deeper understanding of spectroscopic measures of excitons in nanoscale materials. The size dependence of exciton transition energies for a range of organic[30,45] and QD[46–49] materials is plotted in Fig. 5. Measurement of the exciton energy does not directly reveal information that allows us to learn generally about excitons by comparing different materials. For example, size-tunable optical properties derive primarily from the bandgap, not the exciton. The bandgap is the energy difference between occupied and unoccupied orbitals. That provides only a starting point for establishing the excitation energy because, first, the electronic excited-state wavefunction is not accurately written as a one-electron excitation between these orbitals. For example, to develop a theory for calculating electronic spectra Pariser and Parr[50] decided that a method involving antisymmetrized product wavefunctions and configuration interaction was essential. Second, the interactions between electrons in the excited state differ from those for ground-state configurations. There is lower repulsion between electrons in an excited state than in a closed-shell ground state because a pair of electrons can occupy different orbitals. That decreased electron–electron repulsion gives the exciton binding energy. In addition, an associated quantum mechanical effect arises, known as the exchange interaction. Both of these effects are intimately tied to the size of the exciton because that parameter dictates the average electron–electron separation.

The exchange interaction plays a central role in determining the ordering of electronic spin states in any material. An exchange interaction raises the energy of each singlet state and lowers the energy of the three corresponding triplet spin eigenstates. Such a distinction between singlet and multiplet states is a traditional backbone to atomic and molecular spectroscopy. Similarly, the exchange interaction mixes the single-excitation configurations in a QD, evident as a splitting between the bright and dark exciton states at the band edge[47,51,52] (Fig. 6). QDs with wurtzite structure are complicated by crystal field

effects, otherwise the exciton fine structure splitting is determined by the same kind of exchange interaction that splits singlet and triplet states of molecules. As an exciton is spatially compressed by confinement, exchange interactions are increased, as evidenced by larger singlet–triplet splitting. The distinct manifold of states provides an opportunity in spectroscopy to learn about the excited states and electronic structure of nanoscale systems. The challenge, however, for materials such as QDs is that the spectrum is obscured by inhomogeneous line broadening, so specialized techniques are required to probe these states.

The singlet–triplet splittings for the conjugated oligomers[53–56] are closely comparable to those for the aromatic[57] molecule and polyene series[58]. The long-range character of the exchange interaction is evident in the attenuation of the exchange interaction in the polyenes, polyacenes and conjugated oligomers plotted in Fig. 6. If only one-centre exchange integrals contributed to the singlet–triplet splitting, it would diminish as the inverse of the length L of these quasi-one-dimensional excitons (that is the approximation often used for solid state materials). It turns out that the splitting falls off approximately as $L^{1/3}$ for each of these materials, which is a result of long-range exchange interactions, clearly significant over 3 nm. The polyacenes and conjugated oligomers are 'less linear' than the polyenes: in other words the exciton is about twice as wide (compare the chemical structures). That extra width is manifest in the delocalization of the exciton, through molecular orbital coefficients, hence reducing the magnitude of the exchange interaction for any length by approximately a factor of two compared with the corresponding polyene. One can see, therefore, how the exchange interaction (singlet–triplet splitting) is a good measure of exciton size, regardless of the chemical structure of a material. It is in that way that one should think about the CNT data[59] plotted in Fig. 6. The exciton is very long, but an increase in CNT diameter further delocalizes the exciton around the tube, reducing the exchange interaction.

We see that nanoscale materials provide a fascinating intermediate ground between molecular and bulk materials. Interesting spectroscopic properties of excitons, which are often minuscule in bulk materials, are greatly accentuated in nanometre-sized materials and molecules. For example, the electron–hole exchange interaction is of the order of millielectronvolts in bulk semiconductor materials, but is increased 1,000-fold in QDs[51,60–65]. That is still several hundred times smaller than exchange interactions in organic materials that are <10 nm in size (Fig. 6). However, once an exciton in an organic material is as large as that in a CNT, the exchange interaction is reduced to tens of millielectronvolts.

As yet, a number of aspects of the photophysics of CNTs have not been satisfactorily resolved. For example, the reasons underlying the low quantum yield (~10^{-4}) and the fluorescence decay behaviour (~10–200 ps) of the band edge exciton in CNTs are unclear[66], but a closely located triplet state is considered to be a possible contributor. The singlet–triplet splitting for the CNTs is calculated to be of the order of 10 to 40 meV, and is predicted[59], according to calculations based on a tight-binding Hamiltonian, to depend on the inverse of the tube diameter, as shown in Fig. 6. Considering the trend for the other

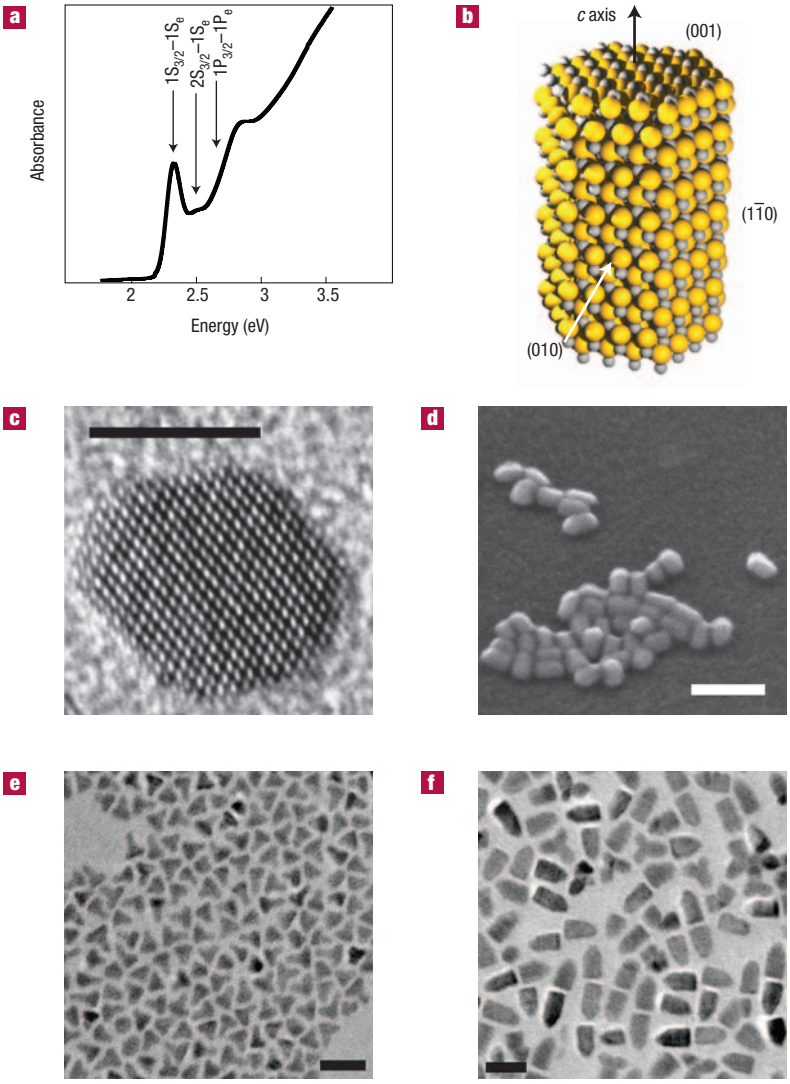

Figure 4 Colloidal CdSe quantum dots. a, An absorption spectrum recorded at 4 K of CdSe QDs with 4.0 nm mean diameter. Hole and electron states associated with excitons seen as the prominent absorption features are labelled according to the assignments of ref. 42. That notation[34] specifies a hole or electron state as $n^*(l, l+2)F$, where n^* labels ground and excited states, l is the minimum orbital quantum number and $F = l + j$ is the total angular momentum quantum number (orbital plus spin), containing F_z from $-F$ to $+F$. Usually just the major contributor out of l or $l+2$, or alternatively just l, is written as S, P, D and so on. That quantum number is associated with the envelope function, usually modelled mathematically as a spherical Bessel function $j_l(x)$. The quantum number j is associated with the Bloch function. For example, the upper valence band of a zinc blende structure has $j = 3/2$ and $j_z = -3/2, -1/2, 1/2, 3/2$. **b**, A structural model of a small, idealized wurtzite nanorod with some crystallographic planes and the direction of the c-axis indicated. **c**, A high-resolution transmission electron micrograph of an individual CdSe wurtzite nanorod, looking down the nanocrystal c-axis. Scale bar corresponds to 5.2 nm. Reprinted from ref. 119. Copyright (2006), with permission from Elsevier. **d**, A scanning-mode electron micrograph of CdSe nanorods. Scale bar corresponds to 50 nm. **e**,**f**, By varying growth conditions a myriad of other shapes can be produced by selective growth of different crystal faces. The scale bars each correspond to 20 nm. Note that the ends of each rod are not identical, as there is no centre of inversion or reflection symmetry in a plane normal to the c axis of the crystal, so asymmetric rods like the bullet-shaped colloids seen in **f** can be grown (P. S. Nair, K. P. Fritz & G. D. Scholes, unpublished data).

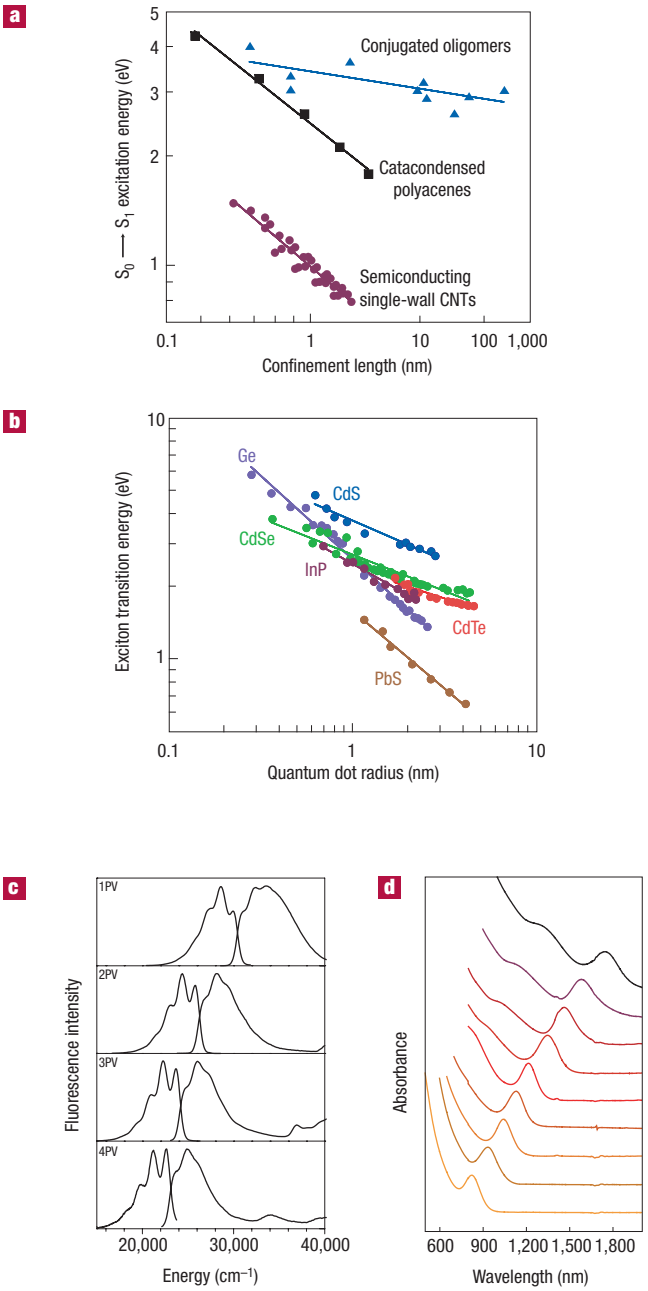

Figure 5 Size dependence of exciton transition energies. Log–log plots of excitation energy versus confinement length (dimension) of the ground and first excited states. For CNTs, the confinement dimension is taken to be the tube diameter. For the other organic materials it is the approximate conjugation length from end to end. **a**, Organic materials. Squares show data for the series of aromatic molecules[45] naphthalene, anthracene, naphthacene, pentacene and hexacene. Triangles indicate data for some oligomers that serve as models for conjugated polymers: methyl-substituted ladder-type poly(p-phenylene) (MeLPPP), poly(2,7-(9,9-bis(2-ethylhexyl)fluorene)) (PF2/6)[53,54], oligofluorenes[56] and oligothiophenes[55]. Data were typically recorded for samples at 80 K. The filled circles show CNT data recorded at ambient temperature[30]. **b**, Size-tuning of excitation energies for various QD materials: Ge[49], calculated using *ab initio* density functional theory using ΔSCF, CdSe, CdS and CdTe (ref. 48), measured at 250 K, PbS (ref. 46), measured at 293 K, and InP (refs 47,61) measured at 10 K. **c**, The size-scaling of conjugated molecules, for example phenylenevinylene (PV) oligomers[120], derives from size-limited delocalization of the molecular orbitals. Absorption and fluorescence spectra are shown as a function of the number of PV repeat units. **d**, In semiconductor QDs, the small size of the nanocrystal compared with the exciton in the bulk material confines the exciton. A result is size-dependent optical properties, as shown for the absorption spectra of PbS quantum dots[46].

organic materials, long-range exchange interactions may modify that predicted size-dependence and magnitude. Experimental observation of this splitting seems to be an important next step.

The basic size-scaling of the dark state/bright state splitting for the range of QDs follows a similar trend to that seen for the organic materials, but the magnitudes of the splitting are substantially smaller. The main reason for that is that the high dielectric constant of QDs attenuates the long-range electron–electron repulsion compared with these organic materials. It is striking that the exchange interactions over the range of materials plotted in Fig. 6 are similar in magnitude for each QD size. Confinement of the QD exciton is in three dimensions, therefore the exchange is predicted to scale as R^{-3}, where R is the QD radius. That is the case for some of the data plotted here, which include a range of experimental observations and good quality calculations. A scaling of $\sim R^{-3}$ is found for bright–dark splitting of CdSe, CdTe and GaAs QDs. Silicon QDs are calculated to show $R^{-2.6}$, whereas the splitting for AgI, InAs and InP scales as R^{-2}, or slightly more weakly. Future work may expose more details of the spectroscopic signatures of the exciton from beneath the inhomogeneously broadened absorption band. An example was reported recently where the dynamics associated with flipping between two QD fine-structure states was measured[67].

A concluding message is that nanoscale materials of vastly different structure and composition can be directly compared through spectroscopic signatures of exciton delocalization. Any effect that is determined by a two-electron integral involving orbitals that constitute the exciton is appropriate, although the exchange interaction seems the obvious choice. Finally we note that in this section we have focused on strongly delocalized excitons. The discussion becomes more complex for consideration of Frenkel excitons.

EXCITON BINDING ENERGY

The exciton binding energy in a quantum confined system can be taken to be the energy difference between the exciton transition energy (optical gap) and the electronic bandgap, as shown in Box 1. The electronic bandgap can be written as the difference between the ionization potential and electron affinity, assuming no structural relaxation of the material or its surroundings[68]. This Coulomb energy, thought of as electron–hole attraction, assumes marked significance in nanoscale materials. In this section we discuss the binding energy of excitons in various materials, aiming to understand how to think about confinement in terms of the prevalence of excitons as elementary excitations. We give further examples that illustrate how the size and binding energy of an exciton can be dynamic, changing considerably from optical absorption to equilibration prior to photoluminescence emission.

In a bulk semiconductor material with high dielectric constant, the exciton binding energy is typically small: 27 meV for CdS, 15 meV for CdSe, 5.1 meV for InP and 4.9 meV for GaAs. Excitons are therefore not a distinctive feature in the spectroscopy of such materials at room temperature, making them

ideal for photovoltaic applications. On the other hand, in molecular materials, the electron–hole Coulomb interaction is substantial—a few electronvolts. In nanoscale materials we find a middle ground where exciton binding energies are significant in magnitude—that is, excitons are important—and they are size-tunable. As a consequence of the size-dependence of the binding energy, delocalization versus localization of the exciton complicates matters. For example, exciton self-trapping (see the following section) in organic materials, such as conjugated polymers, leads to a strongly bound (hundreds of millielectronvolts) exciton. Hence the need to dope conjugated polymer solar cells with electron acceptors, such as other polymers[69], fullerenes[70] or quantum dots[71], to promote charge separation. In a strongly delocalized exciton, free carriers could be photogenerated directly upon excitation of conjugated polymers. The extent to which that occurs is still a matter for debate.

The exciton binding energy in QDs of radii $R \approx 1$–2 nm is in the range 200–50 meV, scaling approximately as $1/R$, according to the size-dependence of the electron–hole Coulomb interaction[60]. A key difference between these inorganic materials and organic materials is dielectric constant. Dielectric constant is central in determining the exciton binding energy because it shields electron–electron repulsions, or equivalently electron–hole interactions. Interestingly, it has been reported that dielectric constant diminishes with size for QDs, further increasing the size effect of the exciton binding energy[60].

The importance of electron–electron interactions in determining the properties of excitons in CNTs has been revealed by quantum chemical calculations[72–74]. The most striking result is the large binding energy, found to be between ~0.3 and 1.0 eV, depending on the chiral index and computational methodology. The remarkable finding is that they are of the order of half the bandgap. Zhou and Mazumdar[74] report the scaling of the binding energy for various CNT types, indicating that the binding energy is greater for smaller tube diameters, as expected. Compelling experimental evidence for a significant exciton binding energy in CNTs has been recently communicated[75,76]. In each case, experimental studies suggested that the exciton binding energy in (8,3) CNTs is ~0.4 eV. Evidence for the existence of excitons in CNTs can also be inferred from a report of phonon sidebands in fluorescence data[32]. In the work reported by Wang *et al.*[75] the energy of the one-photon allowed exciton absorption was compared with the two-photon allowed absorption into a second exciton state and nearby continuum absorption. That direct observation of the exciton transition and the continuum provides a clean measure of the exciton binding energy. In the report of Ma *et al.*[76] the one-exciton state and continuum were detected using ultrafast transient absorption spectroscopy, similarly enabling the exciton binding energy to be deduced.

The situation becomes less clear when the material is disordered or when there is strong coupling between electronic and nuclear degrees of freedom. Organic materials typically exhibit structural disorder and tend to contain torsional motions and related low-frequency vibrations that couple to the exciton. Such a combination of static disorder and electron–vibration coupling disrupts delocalization. That is the trade-off for the great structural diversity in both repeat units and extended bonding patterns found in organic supramolecular assemblies and macromolecules. These ideas have been elucidated in detail for J-aggregates[77], which are well known linear assemblies of dye molecules.

It has taken many years to develop an acceptable understanding of excitons in conjugated polymers that

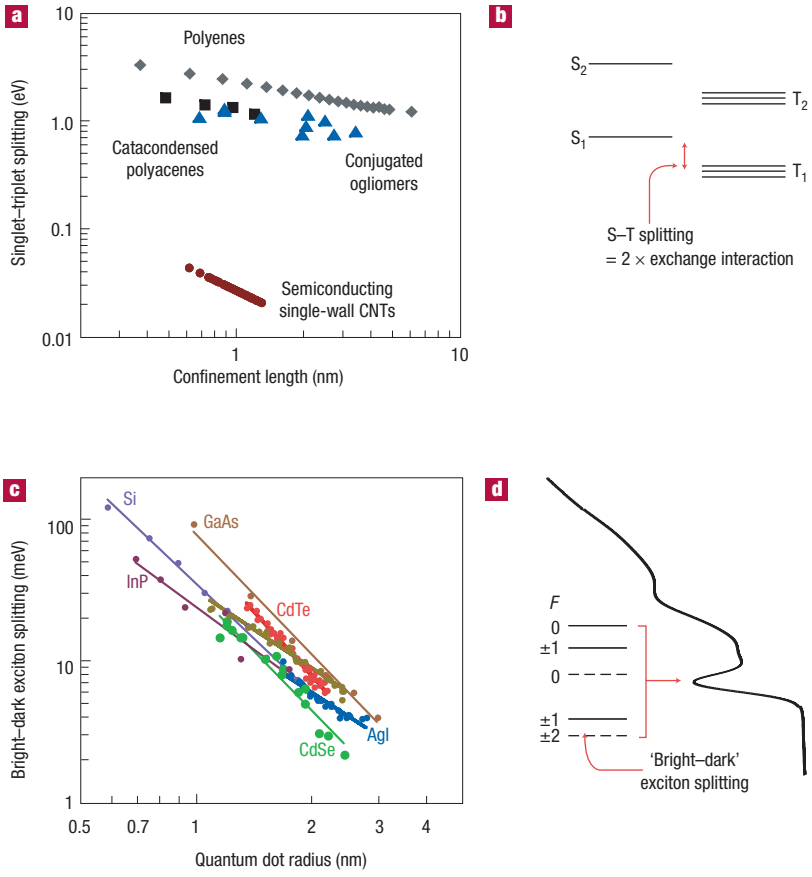

Figure 6 Size dependence of exchange interactions. Log–log plots of singlet–triplet splitting energy versus size. As in Fig. 5, for CNTs the confinement dimension is taken to be the tube diameter; for other organic materials it is the approximate conjugation length from end to end. **a**,The organic materials from Fig. 5, together with calculated singlet–triplet splitting for a series of all-trans polyenes. The diamonds show the results of these time-dependent density functional calculations of polyene excited states[58]. **b**, A typical Jablonskii diagram, indicating that the singlet–triplet splitting is determined by an exchange interaction. That diagram is compared to that for a CdSe quantum dot, shown in **d**, where one considers a manifold of eight states—the exciton fine structure—rather than just four. The splitting between the lowest bright and dark exciton fine structure states is analogous to the singlet–triplet splitting of the organic materials when crystal field splitting is negligible compared with the electron–hole exchange interaction. That is usually not the case for materials with a wurtzite structure, such as CdSe. **c**, Data showing reported bright–dark exciton splitting for a selection of quantum dots: Si (ref. 62; tight-binding calculations), InP (ref. 47; fluorescence line narrowing, measured at 10 K), GaAs (ref. 60; pseudopotential calculations of rectangular nanocrystals), CdTe (ref. 64; fluorescence line narrowing, 10 K, of colloids in glass), AgI (ref. 65; fluorescence line narrowing, 2 K), InAs (ref. 63; fluorescence line narrowing, 10 K), and CdSe(ref. 51; fluorescence line narrowing, 10 K). These data are a combination of experimental results and calculations.

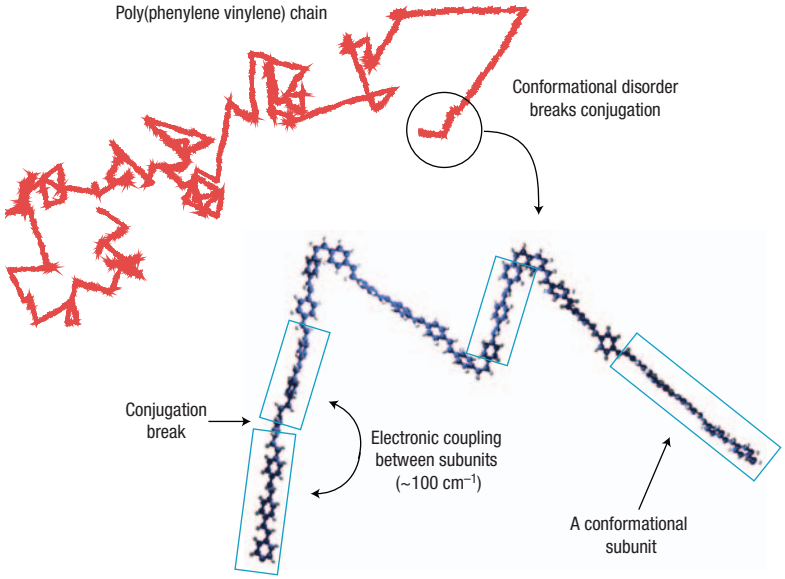

Figure 7 Conformational subunits of conjugated polymers. A typical 'defect cylinder' conformation of a conjugated polymer, poly(phenylene vinylene), is shown in red. Zooming in on a small part of the chain, it is evident that the π-bonds extending over the phenylene vinylene repeat units are frequently disrupted by rotations of sufficient angle to break the conjugation. The result is a series of conformational subunits, outlined conceptually by boxes. This ensemble of chromophores makes up the zero-order picture of the conjugated chain exciton. Long-range Coulomb interactions couple the conformational subunits, as indicated. After light-absorption, energy migration transfers the excitation to a narrow distribution of conformational subunits, from which fluorescence emission is observed.

explains molecular and semiconducting aspects of the materials in the context of their highly disordered structure[20]. The binding energy and precise nature of the excited state (exciton versus polaron-exciton) are still a matter for discussion. We note that coupling to phonons, exciton self-trapping and energy migration can influence the observed binding energy. Electronic structure calculations in conjunction with experiment have proven central for elucidating the properties of excitons in conjugated polymers[78]. Moses *et al.*[79] report that the exciton binding energy can be as low as 60 meV for excitons in poly(phenylene vinylene). The report of Silva *et al.*[80] on poly-6,6′,12,12′-tetraalkyl-2,8-indenofluorene and that of Arkhipov and Bässler[81] should be considered in conjunction with those results. Many other experimental and theoretical reports conclude that the exciton binding energy is 0.3 to 0.6 eV for a range of conjugated polymers. Films differ from isolated polymers owing to interchain interaction effects. The reader is referred to the article by Brédas *et al.*[82] for detailed discussion of the binding energy in conjugated polymers. An important message of that paper is that an interplay between electron–electron and electron–lattice interactions is important in determining a description of conjugated polymer excitons, and hence their binding energies.

The binding energy of the exciton in the B850 ring of LH2 is apparently lowered by 90 meV relative to that in monomeric Bchl, as can be inferred from the energy difference between the 800-nm and 850-nm absorption bands (Fig. 2). Note that B850 is a Frenkel exciton, so the electron and hole are closely associated on each molecule in the aggregate. If the molecules in B850 were sufficiently closely spaced, then charge transfer between Bchl molecules would become important—that is, electron–hole separation. The consequence would be a substantially increased exciton binding energy for essentially the same-sized aggregate.

DISORDER AND COUPLING TO VIBRATIONS

The purely 'electronic' models for describing excitons are modified by the coupling between the exciton and the bath of nuclear motions. That coupling is manifest in spectroscopy as line broadening, Stokes shift and vibronic structure in absorption and photoluminescence spectra[83,84]. The aim of this section is to categorize the important elements of line broadening in nanomaterials, highlight their size dependences and provide some specific examples that give an overall picture of the diverse consequences of disorder and exciton–bath coupling.

Any model for the eigenstates and energies of excitons contains the energy at each repeat unit (molecule, unit cell, atom), known as the site energy, and information on how those repeat units are coupled. In the most general model, each site can accommodate an excitation, an electron or a hole[85]. Clearly both the composition of the eigenstates and the corresponding energies will be affected by energetic disorder in the site energies or couplings. Such disorder is caused by random fluctuations in the positions of atoms[84]. The timescale of those fluctuations is important in delimiting the effects as static (on the timescale of the measurement) or fluctuating. The former gives rise to inhomogeneous line broadening, the latter to homogeneous line broadening[86]. Static disorder is seen as a temperature-independent gaussian line shape in absorption or photoluminescence, whereas homogeneous line broadening can play an important role in trapping an exciton on a fast timescale[87] (femtoseconds to picoseconds).

The interaction between excitons and nuclear motions can introduce time-dependent confinement effects, known as exciton self-trapping, where the exciton becomes trapped in a lattice deformation[87]. Those nuclear motions are contributed by intramolecular vibrations and the environment. Exciton self-trapping occurs through a local collective structural change, connected to random nuclear fluctuations by the fluctuation-dissipation theorem. The resultant exciton is also called a polaron-exciton. Hence the size and electronic make-up of an organic exciton can change markedly on short timescales after photoexcitation (tens of femtoseconds)[13,88]. That is understood as the tendency of molecules to change their equilibrium geometry in the excited state compared with the ground state, which is observed, together with solvation[86], as spectral diffusion. The associated reorganization energy is equal to half the Stokes shift. A very small change in the equilibrium coordinates of many vibrational modes can inspire surprisingly rapid localization of the exciton. In other words, exciton self-trapping is induced by the amplitude of fluctuations as well as their characteristic

timescales. The precise excited state dynamics are dictated by competition between the delocalizing effect of electronic coupling and the localizing influence of electron–phonon coupling.

The LH2 antenna protein (Fig. 2) from purple bacteria provides a clear example of the implications of static disorder at each site in a Frenkel exciton. To understand the optical properties, one must consider the importance of static disorder in the transition energy gaps from ground state to excited state of each Bchl molecule and/or in the electronic coupling[89–91]. The result is that each LH2 complex in an ensemble has a unique absorption spectrum, as shown strikingly in the low-temperature fluorescence excitation spectra of individual LH2 complexes reported by van Oijen *et al.*[92]. Implications are that ensemble measurements must be carefully unravelled to expose the properties and dynamics characteristic of individual light-harvesting complexes. Although static disorder is important, particularly in determining the temperature dependence of spectroscopic data, dynamic electron–vibration coupling also needs to be considered to predict electronic energy transfer rates and to understand ultrafast exciton dynamics. Some insight into the role of electron–vibration coupling can be gathered from the observation that the entire ring of Bchl molecules needs to be considered in a theoretical model to predict correctly the absorption or circular dichroism spectra of B850[17]. Nonetheless, excitation is self-trapped in just tens of femtoseconds so that the exciton size determined by experiments such as pump-probe[93] and time-resolved fluorescence spectroscopy[94] is small enough to cover just small part of the ring, typically three to four Bchl molecules only. The size of an exciton therefore can depend on the timescale on which it is probed.

Conjugated polymers provide another good example where static disorder is significant. By considering single-molecule studies and simulations of the polymer chain it was established that MEH-PPV adopts a fairly ordered defect cylinder chain conformation[95], illustrated in Fig. 7. That work provides an important 'low-resolution' picture of chain disorder. The π-electron system of conjugated polymers is disrupted on shorter length scales by conformational disorder[20]. It has been thought that this disorder impacts the spectroscopy by disrupting the π-electron conjugation along the backbone of the polymer, giving a chain of chromophores known as conformational subunits (Fig. 7). Thus, the optical properties of conjugated polymers are highly dependent on the polymer chain conformation[20,22,96]. Single-molecule studies and site-selective fluorescence studies together provide clear evidence that energy absorbed by a polymer chain is efficiently funnelled to low-energy chromophores along the chain by electronic energy transfer[97].

Recent work has aimed to understand better how to think about conformational subunits and how they define conjugated polymer excitons. Simple considerations of electronic coupling (for example, dipole–dipole coupling) suggest that conformational subunits should be electronically coupled, meaning that a delocalized exciton might be formed by photoexcitation[98–100]. Careful quantum chemical investigations furthermore reveal that it is difficult to define conformational subunits with respect to torsional angles: there is no clear point when the strong interactions that depend on π–π overlap 'switch off' and, even when weak, those interactions are important for defining the nature of the excited states. Beenken and Pullerits[101] conclude that conformational subunits arise concomitantly with dynamic localization of the excitation[102] (exciton self-trapping). An interesting contrast is contributed by the highly ordered polydiacetylene chains investigated by Schott and co-workers[103]. Those molecules resemble an organic semiconductor quantum wire in many respects, therefore sustaining a highly delocalized one-dimensional exciton. Key properties that differentiate these chains from many other conjugated polymers are their structural order on all length scales, their rigid, crystalline environment, and weaker electron–phonon coupling.

QD excitons couple relatively weakly to nuclear motions and the homogeneous line broadening is consequently narrow compared with organic materials, suggesting possible applications of QDs as single-photon sources and 'qubits' for quantum computation. That is perhaps because QDs, and indeed also CNTs, are considerably more rigid and ordered than the flexible structures of organic materials. There are two characteristic types of vibrations in a QD[104]. The higher-frequency mode is that of the longitudinal optical (LO) phonon, which has a frequency that is typically very similar to the frequency known for the corresponding bulk material. For CdSe the LO-phonon mode frequency is 207 cm^{-1}. The radial breathing modes of CNTs[105] are conceptually similar kinds of vibrations. The frequencies of radial breathing modes, however, scale with the CNT diameter d (in nm), according to the empirical relation[106] $\omega = (214.4/d) + 18.7$ cm^{-1}. Coupling of the exciton to vibrations with frequencies greater than thermal energies leads to phonon sidebands in frequency-resolved spectroscopies and quantum beats (oscillations) in ultrafast time domain experiments.

The principal vibrations that contribute to QD line shape are acoustic phonons. In the bulk these are analogous to sound waves travelling through the crystal. Owing to the small size of QDs, the acoustic phonon modes are quantized torsional and spheroidal modes—the motions of an elastic sphere that leave its volume constant. The frequencies of these phonon modes lie in the range 5 to 40 cm^{-1}, depending on the QD size. The exciton–phonon coupling scales as $1/R^2$, where R is the QD radius[104]. Models for phonons in bulk crystals assume the displacements of the modes are small. That makes sense for an infinite-sized crystal, in which coupling between many oscillators limits the amplitude of motion. On the other hand, for nanoscale materials such as QDs, exciton–phonon coupling may be better described by considering aspects of theories developed for molecules.

DYNAMICS OF EXCITONS

The dynamics of excitons have been of interest for many years. Here we give only a glimpse of some

areas topical in nanoscience that characterize each particular material. Photosynthetic proteins provide wonderful model materials for the measurement and investigation of electronic energy transfer. Energy migration in conjugated polymers has been extensively studied, particularly with respect to elucidating the essential differences between dilute solutions and films[97]. Exciton dynamics in CNTs have recently been exposed, so this area is only now emerging. Relaxation dynamics—radiationless as well as radiative relaxation—of highly excited excitons and multiexcitons are a topic of continued interest in QDs.

As introduced in Fig. 2, the light-harvesting complexes in photosynthesis gather incident solar energy and transfer that excitation energy to reaction centres using a series of electronic energy transfer steps. The B850 unit plays an important role in the intra-complex energy funnel for purple bacteria. Examination of B800–B850 resonance energy transfer revealed that excitons are unique in the way they trap excitation energy[17,18]. A surprisingly large spatial and spectral cross-section for donor quenching is achieved through the physical arrangement of the acceptor molecules, together with the fact that the full extent of the exciton density of states can be harnessed to optimize spectral overlap between donor 'emission' and acceptor 'absorption', regardless of the distribution of oscillator strength. This second point is rather subtle, as it is not captured by the dipole approximation for donor–acceptor electronic couplings. The way that a delocalized exciton acts as a unique acceptor in resonance energy transfer may be understood in terms of coupling between exciton transition densities[16–18].

Exciton states are used in photosynthetic light harvesting and redistribution because they substantially increase the absorption cross-section for incident light without the cost of dissipative processes that might result from diffusive trapping of excitation energy absorbed by a weakly coupled aggregate of molecules. Once captured by the exciton manifold, excitation is rapidly trapped in the lowest state. Recent work reveals that such exciton trapping and relaxation is not a simple cascading relaxation process, but can actually involve spatial redistribution, a new picture that was discovered through two-dimensional photon echo spectroscopy[107]. This method opens the possibility of new insights into mechanisms underlying ultrafast dynamics of excitons, because information about electronic couplings between exciton states can be captured in addition to populations.

Similar to conjugated polymers, CNT excitons may migrate along the length of the tube. A possible implication of energy migration is that trap and defect sites along the tube may quench excitation, contributing to the low fluorescence yield. At higher excitation intensities, two excitons on the same CNT may encounter each other and annihilate[108]. Thus multiexciton states are typically short-lived (<100 fs) in organic materials because excitons resident on proximate but spatially distinct parts of a macromolecule or aggregate annihilate efficaciously by a resonance energy transfer mechanism, forming a localized higher electronic state that relaxes rapidly through internal conversion[109,110].

Translational dynamics of excitons are obviously not important in QDs. However, radiationless relaxation processes from higher excited states in QDs to the lowest exciton state have been widely investigated[36]. The electron and hole levels in small QDs, typical of colloidal QDs, are widely spaced compared with the LO-phonon frequency. It was therefore expected that relaxation of the electron and hole, and hence exciton, would be impeded: the phonon bottleneck. In fact, it has been found that the relaxation is very fast in CdSe[111,112]. For CdSe the valence band consists of more closely spaced levels than the conduction band. Bearing this in mind, the fast exciton relaxation has been explained on the basis of an Auger-like process whereby the highly excited electron interacts with the hole through an electronic (coulombic) interaction that enables the electron to relax to its lowest level by scattering the hole deeper into the valence band[111]. Because the valence band has a high density of states, phonon-mediated relaxation of the hole is possible. However, that rationale does not satisfactorily explain the fast exciton relaxation observed in IV–VI QDs, for which the electron and hole states are thought to be approximately equally spaced. Guyot-Sionnest *et al.* have further suggested that surface ligands may play a role in assisting exciton relaxation[113]. Whether independent consideration of the electron and hole relaxations is a good approximation may also be questioned given the significant Coulomb and exchange energies that bind the exciton.

As opposed to most organic materials, QDs can support multiple exciton populations, biexcitons, triexcitons and so on, for times significant compared with the exciton lifetime. Biexcitons in CdSe QDs have recombination times of the order of tens of picoseconds, depending on the QD size[3,112]. Nozik proposed that the unique properties of multiexcitons in QDs could be harnessed to increase the energy conversion efficiency of solar cells[114]. Recently that prediction was confirmed for PbS and PbSe QDs by the striking observations of band-edge exciton yields of >300% when the pump energy is tuned to greater than three times the bandgap[115,116].

OUTLOOK

We emphasize the great strides that have been gained from elucidating size-dependent properties within each class of materials we have reviewed. What are the signatures of nanoscale exciton spectroscopy? As an example we looked at singlet–triplet splitting and its relationship to exciton delocalization (or confinement). The properties of quantum dots stood out from those of the other materials examined; the relatively small magnitude of properties such as the exchange interaction highlights the role of dielectric constant in screening long-range interactions. It is clear, however, that size plays an important role here also, as can be concluded by comparing the singlet–triplet splitting of the majority of organic materials surveyed in Fig. 6 with those calculated for CNTs.

We conclude that an opportunity for nanoscience is that solid-state materials acquire molecular-like spectroscopic features: discrete

transitions, spin state manifolds and so on, allowing for a more detailed examination of the excited states. That, in turn, will provide inspiration for theory, which in the past has focused mostly on bandgaps. Future work will examine more closely how spectroscopy can reveal properties unique to excitons in nanoscale systems. It is likely that our understanding of excited electronic states characteristic of nanomaterials will evolve in a similar manner to our present understanding of the excited states of molecules. Standard approximations and concepts relevant to bulk materials may need to be reconsidered in light of the significant exciton binding energies, exchange interactions, and exciton–vibration couplings apparent in the spectroscopy of nanoscale excitons. Perhaps we need to look back before we go small?

doi: 10.1038/nmat1710

References

1. Friend, R. H. *et al.* Electroluminescence in conjugated polymers. *Nature* **397,** 121–128 (1999).
2. Gregg, B. A. Excitonic solar cells. *J. Phys. Chem. B* **107,** 4688–4698 (2003).
3. Klimov, V. I. *et al.* Optical gain and stimulated emission in nanocrystal quantum dots. *Science* **290,** 314–317 (2000).
4. Koch, S. W., Kira, M., Khitrova, G. & Gibbs, H. M. Semiconductor excitons in a new light. *Nature Mater.* **5,** 523–531 (2006).
5. Elliott, R. J. in *Polarons and Excitons* (eds Kuper, C. G. & Whitfield, G. D.) 269–293 (Plenum, New York, 1962).
6. Knox, R. S. in *Collective Excitations in Solids* (ed. Bartolo, B. D.) 183–245 (Plenum, New York, 1981).
7. McRae, E. G. & Kasha, M. in *Physical Processes in Radiation Biology*, 23–42 (Academic, New York, 1964).
8. Slater, J. C. & Shockley, W. Optical absorption by the alkali halides. *Phys. Rev.* **50,** 705–719 (1936).
9. Hoffmann, R. How chemistry meets physics in the solid state. *Angew. Chem. Int. Edn. Engl.* **26,** 846–878 (1987).
10. Cohen, M. L. Nanotubes, nanoscience, and nanotechnology. *Mater. Sci. Eng. C.* **15,** 1–11 (2001).
11. Cohen, M. L. The theory of real materials. *Annu. Rev. Mater. Sci.* **30,** 1–26 (2000).
12. Tretiak, S. & Mukamel, S. Density matrix analysis and simulation of electronic excitations in conjugated and aggregated molecules. *Chem. Rev.* **102,** 3171–3212 (2002).
13. Brédas, J. L., Beljonne, D., Coropceanu, V. & Cornil, J. Charge-transfer and energy-transfer processes in pi-conjugated oligomers and polymers: a molecular picture. *Chem. Rev.* **104,** 4971–5003 (2004).
14. Sundström, V., Pullerits, T. & van Grondelle, R. Photosynthetic light-harvesting: reconciling dynamics and structure of purple bacterial LH2 reveals function of photosynthetic unit. *J. Phys. Chem. B* **103,** 2327–2346 (1999).
15. Scholes, G. D. & Fleming, G. R. Energy transfer and photosynthetic light harvesting. *Adv. Chem. Phys.* **132,** 57–130 (2005).
16. Scholes, G. D. Long-range resonance energy transfer in molecular systems. *Annu. Rev. Phys. Chem.* **54,** 57–87 (2003).
17. Doust, A. B., Wilk, K. E., Curmi, P. M. G. & Scholes, G. D. The photophysics of cryptophyte light harvesting. *J. Photochem. Photobiol. A. Chem.* (in the press); doi:10.1016/j.jphotochem.2006.06.006.
18. Scholes, G. D., Jordanides, X. J. & Fleming, G. R. Adapting the Förster theory of energy transfer for modeling dynamics in aggregated molecular assemblies. *J. Phys. Chem. B* **105,** 1640–1651 (2001).
19. Rothberg, L. J. *et al.* Photophysics of phenylenevinylene polymers. *Synth. Met.* **80,** 41–58 (1996).
20. Bässler, H. & Schweitzer, B. Site-selective fluorescence spectroscopy of conjugated polymers and oligomers. *Acc. Chem. Res.* **32,** 173–182 (1999).
21. Sariciftci, N. S. (ed.) *Primary Excitations in Conjugated Polymers: Molecular Exciton versus Semiconductor Band Model* (World Scientific, Singapore, 1997).
22. Barbara, P. F., Gesquiere, A. J., Park, S.-J. & Lee, Y. J. Single-molecule spectroscopy of conjugated polymers. *Acc. Chem. Res.* **38,** 602–610 (2005).
23. Köhler, A. *et al.* Charge separation in localized and delocalized electronic states in polymeric semiconductors. *Nature* **392,** 903–906 (1998).
24. Morteani, A. C. *et al.* Barrier-free electron–hole capture in polymer blend heterojunction light-emitting diodes. *Adv. Mater.* **15,** 1708–1712 (2003).
25. Morteani, A. C., Sreearunothai, P., Hertz, L. M., Friend, R. H. & Silva, C. Exciton regeneration at polymeric semiconductor heterojunctions. *Phys. Rev. Lett.* **92,** 247402 (2004).
26. Knibbe, H., Røllig, K., Schäfer, F. P. & Weller, A. Charge-transfer complex and solvent-shared ion pair in fluorescence quenching. *J. Chem. Phys.* **47,** 1184–1185 (1967).
27. Terrones, M., Hsu, W. K., Kroto, H. W. & Walton, D. R. M. Nanotubes: a revolution in materials science and electronics. *Top. Curr. Chem.* **199,** 189–234 (1999).
28. O'Connell, M. J. *et al.* Bandgap fluorescence from individual single-walled carbon nanotubes. *Science* **297,** 593–596 (2002).
29. Ando, T. Excitons in carbon nanotubes. *J. Phys. Soc. Japan* **66,** 1066–1073 (1997).
30. Bachilo, S. M. *et al.* Structure-assigned optical spectra of single-walled carbon nanotubes. *Science* **298,** 2361–2366 (2002).
31. Reich, S., Thomsen, C. & Maultzsch, J. Carbon nanotubes: basic concepts and physical properties (Wiley, New York, 2004).
32. Jones, M. *et al.* Analysis of photoluminescence from solubilized single-walled carbon nanotubes. *Phys. Rev. B* **71,** 115426 (2005).
33. Didraga, C. & Knoester, J. Exchange narrowing in circular and cylindrical molecular aggregates: degenerate versus nondegenerate states. *Chem. Phys.* **275,** 307–318 (2002).
34. Gaponenko, S. V. *Optical Properties of Semiconductor Nanocrystals* (Cambridge Univ. Press, Cambridge, 1998).
35. Alivisatos, A. P. Perspectives on the physical chemistry of semiconductor nanocrystals. *J. Phys. Chem.* **100,** 13226–13239 (1996).
36. Burda, C., Chen, X. B., Narayanan, R. & El-Sayed, M. A. Chemistry and properties of nanocrystals of different shapes. *Chem. Rev.* **105,** 1025–1102 (2005).
37. Weller, H. Colloidal semiconductor Q-particles: chemistry in the transition region between solid state and molecules. *Angew. Chem. Int. Edn Engl.* **32,** 41–53 (1993).
38. Klimov, V. I. (ed.) Semiconductor and metal nanocrystals: synthesis and electronic and optical properties (Marcel Dekker, New York, 2004).
39. Bimberg, D., Grundman, M. & Ledentsov, N. N. *Quantum Dot Heterostructures* (Wiley, Chichester, 1999).
40. Yoffe, A. D. Semiconductor quantum dots and related systems: electronic, optical, luminescence and related properties of low dimensional systems. *Adv. Phys.* **50,** 1–208 (2001).
41. Efros, A. L. & Efros, A. L. Interband absorption of light in a semiconductor sphere. *Sov. Phys. Semicond.* **16,** 772–775 (1982).
42. Ekimov, A. I. *et al.* Absorption and intensity-dependent photoluminescence measurement on CdSe quantum dots: assignment of the first electronic transitions. *J. Opt. Soc. Am. B* **10,** 100 (1993).
43. Rabani, E., Hetenyi, B., Berne, B. J. & Brus, L. E. Electronic properties of CdSe nanocrystals in the absence and presence of a dielectric medium. *J. Chem. Phys.* **110,** 5355–5369 (1999).
44. Yin, Y. & Alivisatos, A. P. Colloidal nanocrystal synthesis and the organic-inorganic interface. *Nature* **437,** 664–670 (2005).
45. Klevens, H. B. & Platt, J. R. Spectral resemblances of cata-condensed hydrocarbons. *J. Chem. Phys.* **17,** 470–481 (1949).
46. Hines, M. A. & Scholes, G. D. Colloidal PbS nanocrystals with size-tunable near-infrared emission: observation of post-synthesis self-narrowing of the particle size distribution. *Adv. Mater.* **15,** 1844–1849 (2003).
47. Micic, O. I. *et al.* Size-dependent spectroscopy of InP quantum dots. *J. Phys. Chem. B* **101,** 4904 (1997).
48. Yu, W. W., Qu, L. H., Guo, W. Z. & Peng, X. G. Experimental determination of the extinction coefficient of CdTe, CdSe, and CdS nanocrystals. *Chem. Mater.* **15,** 2854–2860 (2003).
49. Nesher, G., Kronik, L. & Chelikowsky, J. R. Ab initio absorption spectra of Ge nanocrystals. *Phys. Rev. B* **71,** 35344 (2005).
50. Pariser, R. & Parr, R. G. A semi-empirical theory of the electronic spectra and electronic structure of complex unsaturated molecules. I. *J. Chem. Phys.* **21,** 466–471 (1953).
51. Efros, A. L. *et al.* Band-edge exciton in quantum dots of semiconductors with a degenerate valence band: dark and bright exciton states. *Phys. Rev. B* **54,** 4843–4856 (1996).
52. Leung, K., Pokrant, S. & Whaley, K. B. Exciton fine structure in CdSe nanoclusters. *Phys. Rev. B* **57,** 12291–12301 (1998).
53. Hertel, D. *et al.* Phosphorescence in conjugated poly(para-phenylene)-derivatives. *Adv. Mater.* **13,** 65–70 (2001).
54. Köhler, A. & Beljonne, D. The singlet–triplet exchange energy in conjugated polymers. *Adv. Funct. Mater.* **14,** 11–18 (2004).
55. Wasserberg, D., Marsal, P., Meskers, S. C. J., Janssen, R. A. J. & Beljonne, D. Phosphorescence and triplet state energies of oligothiophenes. *J. Phys. Chem. B* **109,** 4410–4415 (2005).
56. Chi, C. Y., Im, C. & Wegner, G. Lifetime determination of fluorescence and phosphorescence of a series of oligofluorenes. *J. Chem. Phys.* **124,** 24907 (2006).
57. McGlynn, S. P., Azumi, T. & Kinoshita, M. *Molecular Spectroscopy of the Triplet State* (Prentice-Hall, Englewood Cliffs, NJ, 1969).
58. Catalán, J. & de Paz, J. L. G. On the ordering of the first two excited electronic states in all-trans linear polyenes. *J. Chem. Phys.* **120,** 1864–1872 (2004).
59. Perebeinos, V., Tersoff, J. & Avouris, P. Radiative lifetime of excitons in carbon nanotubes. *Nanoletters* **5,** 2495–2499 (2005).
60. Fanceschetti, A. & Zunger, A. Direct pseudopotential calculation of exciton coulomb and exchange energies in semiconductor quantum dots. *Phys. Rev. Lett.* **78,** 915–918 (1997).

61. Fu, H. X. & Zunger, A. InP quantum dots: electronic structure, surface effects, and the redshifted emission. *Phys. Rev. B* **56,** 1496–1508 (1997).
62. Leung, K. & Whaley, K. B. Electron–hole interactions in silicon nanocrystals. *Phys. Rev. B* **56,** 7455–7468 (1997).
63. Banin, U., Lee, J. C., Guzelian, A. A., Kadavanich, A. V. & Alivisatos, A. P. Exchange interaction in InAs nanocrystal quantum dots. *Superlattices Microstruct.* **22,** 559–567 (1997).
64. Lavallard, P. *et al.* Exchange interaction and acoustical phonon modes in CdTe nanocrystals. *Solid State Commun.* **127,** 439–442 (2003).
65. Gogolin, O., Mshvelidze, G., Tsitishvili, E., Djanelidze, R. & Klingshirn, C. Exchange interaction in argentum iodide nanocrystals. *J. Lumin.* **102,** 414–416 (2003).
66. Wang, F., Dukovic, G., Brus, L. E. & Heinz, T. F. Time-resolved fluorescence of carbon nanotubes and its implication for radiative lifetimes. *Phys. Rev. Lett.* **92,** 177401 (2004).
67. Huxter, V. M., Kovalevskij, V. & Scholes, G. D. Dynamics within the exciton fine structure of colloidal CdSe quantum dots. *J. Phys. Chem. B* **109,** 20060–20063 (2005).
68. Yaron, D., Moore, E. E., Shuai, Z. & Brédas, J. L. Comparison of density matrix renormalization group calculations with electron–hole models of exciton binding in conjugated polymers. *J. Chem. Phys.* **108,** 7451–7458 (1998).
69. Halls, J. J. M. *et al.* Efficient photodiodes from interpenetrating polymer networks. *Nature* **376,** 498–500 (1995).
70. Sariciftci, N. S., Smilowitz, L., Heeger, A. J. & Wudl, F. Photoinduced electron transfer from a conducting polymer to buckminsterfullerene. *Science* **258,** 1474–1476 (1992).
71. Huynh, W. U., Dittmer, J. J. & Alivisatos, A. P. Hybrid nanorod–polymer solar cells. *Science* **295,** 2425–2427 (2002).
72. Spataru, C. D., Ismail-Beigi, S., Benedict, L. X. & Louie, S. G. Excitonic effects and optical spectra of single-walled carbon nanotubes. *Phys. Rev. Lett.* **92,** 77402 (2004).
73. Chang, E., Bussi, G., Ruini, A. & Molinari, E. Excitons in carbon nanotubes: an ab initio symmetry-based approach. *Phys. Rev. Lett.* **92,** 196401 (2004).
74. Zhou, H. & Mazumdar, S. Electron–electron interaction effects on the optical excitations of semiconducting single-walled carbon nanotubes. *Phys. Rev. Lett.* **93,** 157402 (2004).
75. Wang, F., Dukovic, G., Brus, L. E. & Heinz, T. F. The optical resonances in carbon nanotubes arise from excitons. *Science* **308,** 838–841 (2005).
76. Ma, Y.-Z., Valkunas, L., Bachilo, S. M. & Fleming, G. R. Exciton binding energy in semiconducting single-walled carbon nanotubes. *J. Phys. Chem. B* **109,** 15671–15674 (2005).
77. Heijs, D. J., Malyshev, V. A. & Knoester, J. Decoherence of excitons in multichromophoric systems: thermal line broadening and destruction of superradiant emission. *Phys. Rev. Lett.* **95,** 177402 (2005).
78. Brédas, J.-L., Cornil, J., Beljonne, D., dos Santos, D. A. & Shuai, Z. Excited-state electronic structure of conjugated oligomers and polymers: a quantum-chemical approach to optical phenomena. *Acc. Chem. Res.* **32,** 267–276 (1999).
79. Moses, D., Wang, J., Heeger, A. J., Kirova, N. & Brazovski, S. Singlet exciton binding energy in poly(phenylene vinylene). *Proc. Natl Acad. Sci.* **98,** 13496–13500 (2001).
80. Silva, C. *et al.* Exciton and polaron dynamics in a step-ladder polymeric semiconductor: the influence of interchain order. *J. Phys.: Condens. Matter* **14,** 9803–9824 (2002).
81. Arkhipov, V. I. & Bässler, H. Exciton dissociation and charge photogeneration in pristine and doped conjugated polymers. *Phys. Status Solidi A* **201,** 1152–1187 (2004).
82. Brédas, J. L., Cornil, J. & Heeger, A. J. The exciton binding energy in luminescent conjugated polymers. *Adv. Mater.* **8,** 447–452 (1996).
83. Lax, M. The Franck–Condon principle and its application to crystals. *J. Chem. Phys.* **20,** 1752–1760 (1952).
84. Sumi, H. Exciton–lattice interaction and the line shape of exciton absorption in molecular crystals. *J. Chem. Phys.* **67,** 2943–2954 (1977).
85. Scholes, G. D., Harcourt, R. D. & Ghiggino, K. P. Rate expressions for excitation transfer. III. An ab initio study of electronic factors in excitation transfer and exciton resonance interactions. *J. Chem. Phys.* **102,** 9574–9581 (1995).
86. Fleming, G. R., Passino, S. A. & Nagasawa, Y. The interaction of solutes with their environments. *Phil. Trans. R. Soc. London A* **356,** 389–404 (1998).
87. Nakajima, S. *The Physics of Elementary Excitations* (Springer, New York, 1980).
88. Franco, I. & Tretiak, S. Electron-vibrational dynamics of photoexcited polyfluorenes. *J. Am. Chem. Soc.* **126,** 12130–12140 (2004).
89. Jimenez, R., Dikshit, S. N., Bradforth, S. E. & Fleming, G. R. Electronic excitation transfer in the LH2 complex of *Rhodobacter sphaeroides*. *J. Phys. Chem.* **100,** 6825–6834 (1996).
90. Alden, R. G. *et al.* Calculations of spectroscopic properties of the LH2 bacteriochlorophyll-protein antenna complex from *Rhodopseudomonas acidophila*. *J. Phys. Chem. B* **101,** 4667–4680 (1997).
91. Jang, S., Dempster, S. E. & Silbey, R. J. Characterization of the static disorder in the B850 band of LH2. *J. Phys. Chem. B* **105,** 6655–6665 (2001).
92. Van Oijen, A. M., Ketelaars, M., Köhler, J., Aartsma, T. J. & Schmidt, J. Unraveling the electronic structure of individual photosynthetic pigment-protein complexes. *Science* **285,** 400–402 (1999).
93. Pullerits, T., Chachisvilis, M. & Sundström, V. Exciton delocalization length in the B850 antenna of *Rhodobacter sphaeroides*. *J. Phys. Chem.* **100,** 10787–10792 (1996).
94. Monshouwer, R., Abrahamsson, M., van Mourik, F. & van Grondelle, R. Superradiance and exciton delocalization in bacterial photosynthetic light-harvesting systems. *J. Phys. Chem. B* **101,** 7241–7248 (1997).
95. Hu, D. *et al.* Collapse of stiff conjugated polymers with chemical defects into ordered, cylindrical conformations. *Nature* **405,** 1030–1033 (2000).
96. Schindler, F. *et al.* Counting chromophores in conjugated polymers. *Angew. Chem. Int. Edn Engl.* **44,** 1520–1525 (2005).
97. Beljonne, D. *et al.* Interchain vs. intrachain energy transfer in acceptor-capped conjugated polymers. *Proc. Natl Acad. Sci.* **99,** 10982–10987 (2002).
98. Chang, R., Hayashi, M., Lin, S. H., Hsu, J.-H. & Fann, W. S. Ultrafast dynamics of excitations in conjugated polymers: a spectroscopic study. *J. Chem. Phys.* **115,** 4339–4348 (2001).
99. Wang, X., Dykstra, T. E. & Scholes, G. D. Photon-echo studies of collective absorption and dynamic localization of excitation in conjugated polymers and oligomers. *Phys. Rev. B* **71,** 45203 (2005).
100. Ruseckas, A. *et al.* Ultrafast depolarization of the fluorescence in a conjugated polymer. *Phys. Rev. B* **72,** 115214 (2005).
101. Beenken, W. J. D. & Pullerits, T. Spectroscopic units in conjugated polymers: a quantum chemically founded concept? *J. Phys. Chem. B* **108,** 6164–6169 (2004).
102. Tretiak, S., Saxena, A., Martin, R. L. & Bishop, A. R. Conformational dynamics of photoexcited conjugated molecules. *Phys. Rev. Lett.* **89,** 97402 (2002).
103. Lécuiller, R. *et al.* Fluorescence yield and lifetime of isolated polydiacetylene chains: evidence for a one-dimensional exciton band in a conjugated polymer. *Phys. Rev. B* **66,** 125205 (2002).
104. Takagahara, T. Electron–phonon interactions and excitonic dephasing in semiconductor nanocrystals. *Phys. Rev. Lett.* **71,** 3577–3580 (1993).
105. Plentz, F., Ribeiro, H. B., Jorio, A., Strano, M. S. & Pimenta, M. A. Direct experimental evidence of exciton–phonon bound states in carbon nanotubes. *Phys. Rev. Lett.* **95,** 247401 (2005).
106. Telg, H., Maultzsch, J., Reich, S., Hennrich, F. & Thomsen, C. Chirality distribution and transition energies of carbon nanotubes. *Phys. Rev. Lett.* **93,** 177401 (2004).
107. Brixner, T. *et al.* Two-dimensional spectroscopy of electronic couplings in photosynthesis. *Nature* **434,** 625–628 (2005).
108. Valkunas, L., Ma, Y.-Z. & Fleming, G. R. Exciton–exciton annihilation in single-walled carbon nanotubes. *Phys. Rev. B* **73,** 115432 (2006).
109. De Schryver, F. C. *et al.* Energy dissipation in multichromophoric single dendrimers. *Acc. Chem. Res.* **38,** 514–522 (2005).
110. Sternlicht, H., Nieman, G. C. & Robinson, G. W. Triplet–triplet annihilation and delayed fluorescence in molecular aggregates. *J. Chem. Phys.* **38,** 1326–1335 (1963).
111. Klimov, V. I., McBranch, D. W., Leatherdale, C. A. & Bawendi, M. G. Electron and hole relaxation pathways in semiconductor quantum dots. *Phys. Rev. B* **60,** 13740–13749 (1999).
112. Klimov, V. I., Mikhailovsky, A. A., McBranch, D. W., Leatherdale, C. A. & Bawendi, M. G. Quantization of multiparticle Auger rates in semiconductor quantum dots. *Science* **287,** 1011–1013 (2000).
113. Guyot-Sionnest, P., Wehrenberg, B. & Yu, D. Intraband relaxation in CdSe nanocrystals and the strong influence of the surface ligands. *J. Chem. Phys.* **123,** 74709 (2005).
114. Nozik, A. J. Quantum dot solar cells. *Physica E* **14,** 115–120 (2002).
115. Schaller, R. D. & Klimov, V. I. High efficiency carrier multiplication in PbSe nanocrystals: Implications for solar energy conversion. *Phys. Rev. Lett.* **92,** 186601 (2004).
116. Ellingson, R. J. *et al.* Highly efficient multiple exciton generation in colloidal PbSe and PbS quantum dots. *Nanoletters* **5,** 865–871 (2005).
117. Scholes, G. D., Ghiggino, K. P., Oliver, A. M. & Paddon-Row, M. N. Through-space and through-bond effects on exciton interactions in rigidly linked dinaphthyl molecules. *J. Am. Chem. Soc.* **115,** 4345–4349 (1993).
118. Curutchet, C. & Mennucci, B. Toward a molecular scale interpretation of excitation energy transfer in solvated bichromophoric systems. *J. Am. Chem. Soc.* **127,** 16733–16744 (2005).
119. Fritz, K. P. *et al.* Structural characterization of CdSe nanorods. *J. Cryst. Growth* **293,** 203–208 (2006).
120. Gierschner, J., Mack, H.-G., Lüer, L. & Oelkrug, D. Fluorescence and absorption spectra of oligophenylenevinylenes: vibronic coupling, band shapes, and solvatochromism. *J. Chem. Phys.* **116,** 8596–8609 (2002).

Acknowledgements

G.D.S. thanks G. J. Wilson for introducing him to excitons. He acknowledges funding from the Natural Sciences and Engineering Research Council of Canada and the A. P. Sloan Foundation. G.R. acknowledges funding through the Photochemistry and Radiation research program of the US Department of Energy, Office of Science, Office of Basic Energy Sciences, Chemical Sciences, Geosciences and Biosciences (DoE contract DE-AC36-99G010337).
Correspondence should be addressed to G.D.S.

CORRIGENDUM

EXCITONS IN NANOSCALE SYSTEMS

GREGORY D. SCHOLES AND GARRY RUMBLES

Nature Materials **5,** 683–696 (2006).

In this Review Article, the spelling of the first author's name in ref. 74, and in the citation of this reference within the text on page 691, was incorrect. It should have read Zhao.